CHEMISTRY OF MATERIALS

ARTICLE

pubs.acs.org/cm

Lattice Strains in the Ligand Framework in the Octahedral Metal Cluster Compounds as the Origin of Their Instability

Elena Levi* and Doron Aurbach

Department of Chemistry, Bar-Ilan University, Ramat-Gan, Israel 52900

Supporting Information

ABSTRACT: The bond description for cluster compounds is commonly based on the molecular orbital diagrams, where the whole material is characterized by the specific electron population at various energetic levels. In contrast, this work is focused on the distribution of valence electrons between different liganding atoms, calculated first for a wide variety of octahedral metal cluster compounds (mainly Mo_6 and Re_6 chalcohalides) by the bond valence model. This distribution was found to be extremely nonuniform for most of the materials; it depends mostly on the ligand distances from the cluster center: The closer the ligand to the center, the higher is its charge (defined as its bond valence sum). To explain these results, a new model for the electrostatic interactions in the cluster compounds was proposed: The octahedral metal cluster with high polarizing power creates a strong electrostatic field, in which the adjacent separate anions behave as a part of a continuous dielectric medium, adjusting their charge to the distance from the cluster center. The valence violations related to this adjustment are the source of the material instability. Moreover, the bond valence analysis allows for the unveiling of the stabilization mechanisms existing in this type of cluster compounds. It was shown that the formation of mixed chalcohalides with an unusual anion arrangement, and chalcogen linkers with a reduced oxidation state, decreases the valence violation on the ligands. This work also illustrates additional ways of material stabilization, such as ion insertion inside the clusters or into the interstitials between the clusters, an increase in the number of inner ligands from 8 to 12, as well as increasing the connectivity of the structural units, $Me_6X_8L_6$ and $Me_6X_{12}L_6$ (Me is the transition metal; X and L are internal and outer ligands, respectively).

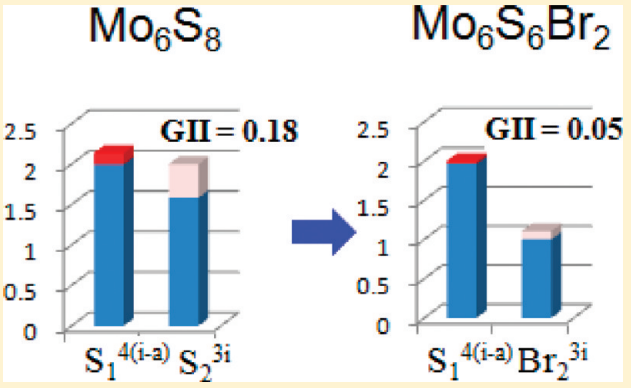

KEYWORDS: cluster compounds, bond valences, lattice strains, material stability

INTRODUCTION

The term "metal cluster" was introduced by Cotton[1] in 1964 to define the groups of atoms with metal−metal bonds. Nowadays, metal cluster compounds, especially those with octahedral clusters, are the subject of intensive studies because of their remarkable physical (catalytic, electrical, magnetic, spectroscopic) properties.[2−7] The well-known example is superconductive Chevrel phases,[3] which are also used as cathodes for rechargeable Mg batteries[4] because of their unique ionic mobility.[5] Another example is the $Mo_6S_3I_6$ nanowires with a wide spectrum of molecular-scale functionality.[6] The studies of the cluster compounds are not related only to the field of inorganic chemistry but rather to materials science in general: Chalcogen or halogen ligands can be substituted for organic groups giving rise to a wide variety of organo-metallic hybrids.[2,7] In spite of the great previous efforts to understand the chemical bonding in these unusual materials,[2,8] this work describes for the first time the effect of the unusually high ligand polarization in the cluster field, evident from the extremely nonuniform distribution of the anion charge around the clusters. It will be shown that this distribution affects greatly the material stability.

In solids, the octahedral clusters of transition metals, Me, form two structural units, $Me_6X_8L_6$ and $Me_6X_{12}L_6$ (Figures 1a and b), where the internal and outer (apical or terminal) ligands (X and L, respectively) are presented typically by chalcogens and/or halogens. Because of their high electron deficiency, clusters of Sc, Sr, Zr, or Nb are often stable only in the presence of an additional atom (Z = metal or nonmetal) or atomic groups in the cluster center (Figure 1c).[9] The L component may be relatively easily substituted for groups like CO, CN, or PEt_3.[2,7] The octahedral clusters surrounded by ligands may exist in solids as separate molecules, or be linked to each other and to additional ions or molecules. As a result, the cluster compounds show a wide variety of structural types with a whole spectrum of physical properties. Bonding (and the physical properties) in these compounds depends not only on the metal−metal and cluster-ligand interactions, but also on the connectivity between the structural units and their relationship with additional ions or molecules. For instance, compounds with a high concentration of nonmetallic

Received: December 20, 2010
Revised: February 13, 2011
Published: March 04, 2011

dx.doi.org/10.1021/cm103617e | *Chem. Mater.* 2011, 23, 1901–1914

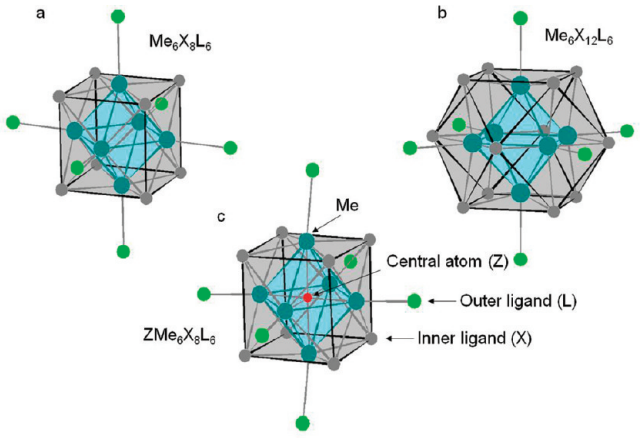

Figure 1. Three types of structural units, with face- (a) and edge-bridge (b) arrangement of the inner ligands, and with an additional atom in the cluster center (c).

atoms (X and L) and a large separation between the clusters are normally insulators,[10] while metal-rich Chevrel phases, $M_xMo_6X_8$ (M = metal, X = S, Se, Te), with additional Mo−Mo bonding between the clusters, are superconductors[3] and unique ionic conductors.[5] However, even in Chevrel phases, within the same structural type, the electronic and ionic transports differ drastically for various compositions because of the different interactions between the Mo_6X_8 hosts and the M-cation guests located between the Mo_6X_8 blocks (Crystal structure of Chevrel phases is presented in the Supporting Information, Figure 1S).[3,5b,5c]

Recently we have shown that simple bond valence calculations are very effective to characterize the cation insertion in Chevrel phases, in particular, to describe the geometry of the available sites and the possible routes for cation transport,[5b,c] as well as to estimate the lattice strains related to this process.[11] The calculation method is based on crystallographic data solely; it utilizes a fundamental relation between the ion bond valence, S_{ij}, and the bond length, R_{ij}:[12]

$$S_{ij} = \exp[(R_0 - R_{ij})/b] \quad (1)$$

where R_0 and b are the empirical constants: R_0 is a tabulated[13] bond valence parameter for the "cation-anion" pairs, while b is usually taken to be 0.37 Å.

The bond valence model was successfully applied not only for common ionic solids but also for coordination compounds,[14] mostly for the determination of the cation oxidation state, V, which can be defined as the bond valence sum (BVS):[12]

$$V = \sum S_{ij} \quad (2)$$

In our previous work[11] devoted to Chevrel phases, we did not restrict the calculations to cations, but performed a full bond valence analysis to study the charge distribution on the chalcogen ligands around the Mo_6-cluster as well. It was found that this distribution is extremely nonuniform for most of these compounds, that is, the bond valence sum of chemically identical but crystallographically different anions differs significantly from their formal oxidation state (−2) (Supporting Information, Figure 2S). Such valence violations are commonly assigned to lattice strains.[12] In fact, existence of strains in the anion framework around the Me_6-clusters was suggested in the previous studies[2b,15] based on the analysis of the interatomic distances. Corbett[15] even introduced a special term "matrix effect". The latter was defined as a steric conflict between strong Mo−X intercluster bonding in Chevrel phases and closed-shell anion repulsion. The attempts were made to correlate the lattice strains to physical properties of cluster compounds, such as chemical reactivity of structural blocks[2b] or material stability.[15]

However, these studies were not continued, maybe because of the absence of clear quantitative characteristics of the lattice strains, which were found later in the framework of the bond valence model.[12] In our previous work[11] we correlated the valence violations to instability of Chevrel phases, but the main questions remained unanswered: What is the origin of the valence violations? Do they exist also in other cluster-containing compounds? If this is the case, the effect of violated ligand charges should have a great impact on the material structure and its physical properties, especially on the material stability.

Thus, the aim of this paper is to study the distribution of the anion charges (defined as their bond valence sums) and the factors affecting this distribution for a wide variety of cluster compounds. The study is based on the calculations by the bond valence model.[12] The results are used to explain the structural peculiarities of the cluster compounds, for example, the formation of mixed chalcohalides with anion ordering or chalcogen cluster linkers with reduced valence. Additionally, we will correlate the valence violations found for the ligands to material instability. This work is focused mainly on the chalcohalides with Mo_6 and Re_6 clusters, while compounds with other clusters are presented for comparison.

BOND VALENCE METHOD FOR CLUSTER COMPOUNDS (MODEL I)

The calculation method[12] in its application to cluster compounds was described in detail in ref 11. Here we point out the basic concepts of the method. To characterize the metal−metal bonding in the clusters, we introduced a bond valence parameter[11] based on the so-called VEC (Valence Electron Count or sum of electrons involved in the cluster bonding), m. For compounds composed of Me_6-clusters, T-ligands (a generic label for X and L), and additional M-cations, m is defined[3] as the sum of the valence electrons of the six Me atoms and x M^{n+} cations minus the number of the valence electrons of the ligands. For instance, for Chevrel phases, $M^{n+}{}_xMo_6X_8$, $m = 6 \times 6 + nx - 2 \times 8$. Since nx for these compounds may vary from 0 to 4, the m values lay in the range of 20 to 24.[3] In contrast to Chevrel phases, the VEC for other Me_6-cluster compounds is constant and equal to 24 and 16 for Me metals with 6 and 5 valence electrons, respectively (Nb_6I_{11} with VEC = 19 is an exception) (Table 1).

The electrons related to the VEC are distributed among all the Me−Me bonds. For instance, in Chevrel phases each Mo atom is connected to five Mo atoms (four bonds within individual Mo_6-clusters plus an additional bond between neighboring clusters), with bond lengths, R_{ij}, which can be found from the atomic coordinates. Thus, we can use five eqs 1, which correlate the unknown bond valence strengths, S_{ij}, with known crystallographic R_{ij} data. In addition, according to eq 2, the sum ΣS_{ij} for the five metal−metal bonds is equal to the Mo electron number, $m/6$. By solving these six equations, we can easily determine the six unknowns, S_1, S_2, S_3, S_4, S_5, and $R_0{}'_{Me-Me}$ (bond valence parameter for a given compound).

The calculations of the anion charge were performed in two steps. First, the valences for all the cation bonds were calculated based on the formal cation oxidation state and the "cation-anion"

dx.doi.org/10.1021/cm103617e |Chem. Mater. 2011, 23, 1901–1914

Table 1. Calculated Bond Valence Parameters and Global Instability Indexes (GII) of the Cluster Compounds Studied in This Work

compound	m	$R_0'_{Me-Me}$ Å	$R_0'_{Me-Se}$ Å (2.35)	$R_0'_{Me-Se}$ Å (2.49)	$R_0'_{Me-Te}$ Å (2.69)	$R_0'_{Me-F}$ Å (1.81)	$R_0'_{Me-Cl}$ Å (2.28)	$R_0'_{Me-Br}$ Å (2.43)	$R_0'_{Me-I}$ Å (2.64)	$R_0'_{Me-T}$ Å	$R_0'_{Me-T}$ Å average (Tab)	GII	structural data ref.
Mo_6S_8	20	2.666	2.203									0.18	
$SnMo_6S_8$	22	2.656	2.181								2.45(2.45)	0.07	3a
$GdMo_6S_8$	23	2.646	2.164								2.53(2.53)	0.08	
$CsMo_{12}S_{14}$	22.5	2.635	2.185								2.892(2.89)	0.06	16a
Mo_6Se_8	20	2.659		2.335								0.13	
Mo_6Te_8	20	2.667			2.534							0.13	3a
Mo_6Cl_{12}	24	2.604					2.124					0.24	16b
$Cu_2Mo_6Cl_8Cl_6$	24	2.605					2.123				1.853(1.85)	0.18	
$Cu_2Mo_6Br_8Br_6$	24	2.628						2.257			1.969(1.99)	0.20	16c
$Cu_2Mo_6I_8I_6$	24	2.672							2.450		2.129(2.16)	0.23	
$Cs_2Mo_6Br_8Br_6$	24	2.635						2.262			3.036(2.95)	0.30	16d
$Cs_2Mo_6I_8I_6$	24	2.679							2.453		3.146(3.18)	0.34	
$NaMo_6Br_8Br_5$	24	2.633						2.259			2.346(2.33)	0.23	
$AgMo_6Br_8Br_5$	24	2.635						2.258			2.212(2.22)	0.23	16e
$Mo_6S_6Br_2$	22	2.670	2.181					2.255				0.05	3b
$Mo_6Br_6S_3$	24	2.646	2.150					2.248				0.18	16f
$Mo_6Cl_{10}Se$	24	2.616					2.122			2.167		0.15	16g
$Cs_4Mo_6Br_{12}S_2$	24	2.631								2.271	2.959(2.98)	0.26	16h
$(TBA)_2Mo_6Cl_8Cl_6$	24	2.602					2.119	2.256					
$(TBA)_2Mo_6I_8I_6$	24	2.683							2.450				
$(TBA)_2Mo_6Cl_8F_6$	24	2.592				1.732	2.123						17a
$(TBA)_2Mo_6Cl_8Br_6$	24	2.603					2.120	2.248					
$(TBA)_2Mo_6Cl_8I_6$	24	2.616					2.126		2.452				
$(TBA)_2Mo_6Br_8F_6$	24	2.615				1.740		2.262					17b
$(TBA)_2Mo_6I_8F_6$	24	2.650				1.733			2.441				
$(TBA)_2Mo_6I_8Cl_6$	24	2.664					2.120		2.436				17c
$(TBA)_2Mo_6I_8Br_6$	24	2.670						2.250	2.443				
$(PNP)_2Mo_6I_8Cl_6$	24	2.654					2.119		2.422				

compound	m	$R_0'_{Me-Me}$ Å	$R_0'_{Me-Se}$ Å (2.37)	$R_0'_{Me-Se}$ Å (2.50)	$R_0'_{Me-Te}$ Å (2.70)	$R_0'_{Me-Cl}$ Å (2.23)	$R_0'_{Me-Br}$ Å (2.45)	$R_0'_{Me-T}$ Å	$R_0'_{Me-T}$ Å average (Tab)	GII	structural data ref.
$Cs_{10}Re_6S_{14}$	24	2.627	2.227						2.836(2.89)	0.26	18a
$Cs_6Re_6S_{12}$	24	2.627	2.224						2.940(2.89)	0.45	18b
$Rb_4Re_6S_{12}$	24	2.626	2.233						2.611(2.70)	0.18	18c
$Rb_4Re_6S_{13}$	24	2.607	2.241						2.644(2.70)	0.19	18d
$Cs_4Re_6S_{13}$	24	2.627	2.241						2.787(2.89)	0.21	18e
$Cs_4Re_6S_{13.5}$	24	2.619	2.234						2.842(2.89)	0.18	
M-$Ba_2Re_6S_{11}$	24	2.624	2.230						2.685(2.77)	0.20	18f
R-$Ba_2Re_6S_{11}$	24	2.625	2.230						2.688(2.77)	0.21	18g
R-$Eu_2Re_6S_{11}$	24	2.621	2.236						2.574(2.53)	0.15	
$Cs_6Re_6Se_{15}$	24	2.605	2.223						2.886(2.89)	0.32	18h
$Cs_6Re_6Se_{15}$	24	2.633		2.344					3.001(2.98)	0.32	18i
$Cs_4Re_6Se_{13}$	24	2.638		2.327					2.914(2.98)	0.24	18d
$Rb_4Re_6Se_{13}$	24	2.644		2.346					2.680(2.81)	0.18	
$K_4Re_6Se_{12}$	24	2.644		2.355					2.627(2.72)	0.18	
$Tl_4Re_6Se_{12}$	24	2.635		2.343					2.578(2.70)	0.09	18j

dx.doi.org/10.1021/cm103617e |*Chem. Mater.* 2011, 23, 1901–1914

Table 1. Continued

compound	m	$R_0'_{Me-Me}$ Å	$R_0'_{Me-Se}$ Å (2.37)	$R_0'_{Me-Se}$ Å (2.50)	$R_0'_{Me-Te}$ Å (2.70)	$R_0'_{Me-Cl}$ Å (2.23)	$R_0'_{Me-Br}$ Å (2.45)	$R_0'_{Me-T}$ Å	$R_0'_{Me-T}$ Å average (Tab)	GII	structural data ref.
Re_6Te_{15}	24	2.676			2.506				2.746 (2.76)	0.22	19a
$Re_6Se_8Te_7$	24	2.638		2.358	2.542				2.716(2.76)	0.25	19b
$Re_6S_8Br_2$	24	2.591	2.237				2.260			0.12	19c
$Re_6Se_8Br_2$	24	2.622		2.359			2.257			0.12	19d
$Re_6Se_8Cl_2$	24	2.633		2.361		2.123				0.24	19e
$Re_6Se_7Br_4$	24	2.616					2.261	2.357		0.07	19f
$Re_6Se_4Cl_{10}$	24	2.605				2.123		2.303		0.30	19g
$Re_6S_4Br_{10}$	24	2.609						2.324		0.25	19h

compound	m	$R_0'_{Me-Me}$ Å	$R_0'_{Me-Cl}$ Å	$R_0'_{Me-Br}$ Å	$R_0'_{Me-I}$ Å	$R_0'_{Me-T}$ Å average	GII	structural data ref.
$(TBA)_2W_6Cl_8Cl_6$	24	2.606	2.142					
$(TBA)_2W_6Br_8Br_6$	24	2.635		2.280				20
$(TBA)_2W_6I_8I_6$	24	2.671			2.462			
Nb_6I_{11}	19	2.759			2.506		0.18	21
$K_4Nb_6Cl_{18}$	16	2.762	2.219			2.496(2.52)	0.05	22a
$Li_2Nb_6Cl_{16}$	16	2.769	2.201			1.895(1.91)	0.06	22b
$LiNb_6Cl_{15}$	16	2.769	2.207			1.849(1.91)	0.08	22c
Sc_7CoI_{12}	18	?			2.592	2.617(2.59)	0.09	23a
Zr_6CoCl_{15}	I8	?	2.298				0.08	23b

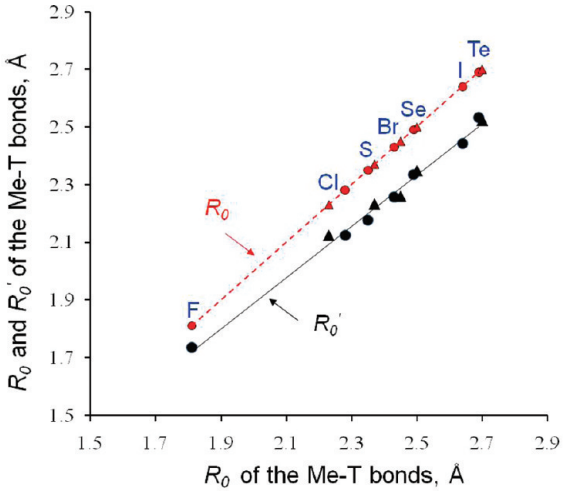

Figure 2. Comparison between tabulated R_0 (in red) and calculated R_0' (in black) bond valence parameters for the Me−T and Me(cluster)−T bonds, respectively (For R_0 Me is an individual cation in common ionic compound, while for R_0' Me is one of the cluster atoms). R_0' are the average data of Table 1 for the Mo_6 and Re_6-cluster compounds (marked by circles and triangles, respectively).

distances in the crystal structure. For instance, in Chevrel phase, $SnMo_6S_8$, Mo and Sn cations are bonded to five and eight sulfur anions, respectively.[3] Using the Mo−S and Sn−S distances,[3] the oxidation state of Mo and Sn ($+2^1/_3$ and +2, respectively), and eqs 1 and 2, we can calculate the valences, S_{ij}, and the individual bond valence parameters, R_0', for the Mo−S and Sn−S bonds in $SnMo_6S_8$.

The calculated bond valence parameters for a variety of cluster compounds are presented in Table 1. Structural data for the valence calculations can be found in refs 3a,16−23. Note that a comparison of R_0' with the tabulated[13] parameters, R_0, provides additional information on bonding (In Table 1, the tabulated R_0 values are given in parentheses). For example, obviously lower values of R_0' for the Me−T bonds in the cluster compounds as compared to the tabulated R_0 (Figure 2) testify to significantly stronger interactions between cluster atoms and their ligands than those for individual Me cations in common ionic compounds. As can be expected, the difference $R_0 - R_0'$ increases for larger and more polarizable anions (More detailed discussion of factors affecting the bond valence parameters for the Me−Me and Me−T bonds in Chevrel phases can be found in our previous work[11]).

In contrast, interactions between anions and additional M-cations located between the Me_6T_8 blocks should be identical to those of common solids (Compare, e.g., $R_0'_{M-T}$ for MMo_6S_8 (M = Sn, Gd), $CsMo_{12}S_{14}$, or $Cu_2Mo_6Cl_{14}$ with the tabulated values). For the M−T bonds, the difference $R_0 - R_0'$ is commonly related to the steric strains between the M-cations and their anion environment. In the previous work[11] we have shown that insertion of such big cations like Ba^{2+} in the relatively rigid anion framework of Chevrel phases results in high steric strains. Thus, the lattice constraints associated with M−T bonding may be also responsible for the material instability. To take them into account, we should to use the R_{0M-T} values instead of $R_0'_{M-T}$. However, in this study we are interested in the anion charge distribution around the clusters. It can be shown than the replacement of R_{0M-T} by $R_0'_{M-T}$ has negligible effect on this distribution, but disturbs the balance of the bond valence sums (see Supporting Information, Figure 2S). Thus, the use of

individual $R_0'_{M-T}$, convenient for each compound, provides a clear advantage in this case: The calculations can be easily verified by the charge balance.

The next step was the calculation of the bond valence sums, ΣS_{ij}, for all the anions, where S_{ij} are the values found in the previous step. For instance, in $SnMo_6S_8$ there are two crystallographically different types of sulfur ions. The first type, S_1 (general position in the space group $R\bar{3}$), is bonded to four Mo and one Sn atoms (valences of 0.507, 0.483, 0.407, 0.365, and 0.182 vu, respectively), while the second type, S_2 (position on the $\bar{3}$ symmetry axis), is coordinated by three Mo and one Sn (valences of 0.570, 0.570, 0.570, and 0.459 vu, respectively). Thus, the bond valence sums are equal to 1.944 vu for S_1 and 2.169 vu for S_2. The formula unit includes 6 S_1 atoms and 2 S_2 atoms, while their total negative charge, obtained in the calculations and equal to 16.002 vu, is very close to the theoretical value of 16 vu. The close values show the correct valence balance in the crystal structure.

The nonuniform anion charge is expected to impart material instability, which can be characterized by the global instability index (GII):[12]

$$\mathrm{GII} = \langle(\sum S_{ij} - V_i)^2\rangle^{1/2} \quad (3)$$

Here, the average is taken over all the atoms in the formula unit. It is commonly accepted[12] that GII > 0.20 vu corresponds to unstable material. The calculated GII for a variety of cluster compounds are presented in Table 1. The details of the bond valence calculations for all the materials under study can be found in the Supporting Information.

RESULTS AND DISCUSSION

Nonuniform Charge Distribution on the Ligands around the Me_6-Clusters. *Ionic Model II: Me_6-Cluster As a Virtual Polyvalent Cation.* In the previous work,[11] it was shown that the nonuniform charge distribution for the X_1 and X_2 anions in Chevrel phases is related to their different linkage to the Me_6-cluster. In addition, one can think that the violation of the valence sum rule is related rather to the electron distribution inside the cluster than to its interactions with the ligands. To clarify the role of the linkage and the internal structure of the Me_6-cluster on the anion charge distribution obtained in our calculations, let us change the bond valence model and treat the entire cluster as a single polyvalent Me_6-cation located in the cluster center (Model II). In contrast to the usual ionic model (Model I) described above, in such a presentation, the linkage of all the anions to the Me_6-cation is the same; the influence of the internal cluster structure is excluded, and the difference between the ligand charges may result only from different anion distances from the cluster center, Me_6—X.

For subsequent discussion it is important to note that the radius of this virtual cation is relatively small. It can be estimated by a comparison of the Me—X and Me_6—X distances in the same compound. For instance, in Mo_6S_8, the length of the minimal Mo—S bond is equal to 2.43 Å, while the minimal Mo_6— S distance is 2.93 Å. For Mo_6Cl_{12} these distances are 2.45 and 3.00 Å, respectively. Similar values can be obtained for the Re_6-clusters (e.g., in $Re_6S_8Br_2$, the lengths of the minimal Re—S and Re_6—S bonds are equal to 2.38 and 2.91 Å, respectively). Thus, the radius of the Mo_6 or Re_6-cation is only ~0.5 Å larger than that of the standard Mo or Re cation (For the Nb_6-cation this difference is about 0.7 Å). Because of the relatively small radius, r (~ 1.3 Å for Mo_6 or Re_6 and ~1.5 Å for Nb_6) and the enormous charge, q (12 e in Mo_6Cl_{12}, 16 e in Mo_6S_8, 18 e in $Re_6S_8Br_2$, 11 e in Nb_6I_{11}, and 14 e in $K_4Nb_6Cl_{18}$), such a cation should have an extremely high polarizing power, q/r^2: 7.1 e/Å^2 in Mo_6Cl_{12}, 9.5 e/Å^2 in Mo_6S_8, 10.7 e/Å^2 in $Re_6S_8Br_2$, 4.9 e/Å^2 in Nb_6I_{11}, and 6.2 e/Å^2 in $K_4Nb_6Cl_{18}$ (For comparison, the polarizing power of Mg^{2+} and Ti^{4+} cations is equal to 3.7 and 9.8 e/Å^2, respectively).

Figure 3a shows that both models I and II result in similar charge distribution on the X_1 and X_2 anions in Chevrel phases. For a variety of cluster compounds with a large separation between the clusters, the similarity is rather qualitative than quantitative (Figure 3b): For both the models, the valence input of the Me—T bonds (cluster electron donation) into the anion charge (bond valence sum) decreases exponentially with the ligand distance from the cluster center, but for model II this decrease is more dramatic: The separation of the outer L ligands from the Me_6-cation is too high for appreciable Me_6—L bonding. This limitation of model II can be avoided by refining the b-parameter in eq 1. As was shown by Adams,[24] the b-values increase with the difference between the anion and the cation softness. According to the high cluster polarizability (see below), a softness of the virtual Me_6-cation should be also very high. In fact, for b close to 1 Å, Model II gives the results, which are similar to those of Model I (Figure 3c. The details of the combined refinement of the R_0' and b parameters can be found in the Supporting Information). As can be seen, the fitting is almost perfect for $Cu_2Mo_6T_{14}$ (T = Cl, Br, I) and $K_4Nb_6Cl_{18}$, while for $Re_6S_4Br_{10}$ and $Cs_6Re_6Se_{15}$ there is a nonsystematic shift between the curves.

It should be emphasized that, to avoid the uncertainty in the b constant, we did not used model II in subsequent calculations. However, the similar results obtained by the two models confirm their validity. Moreover, based on model II, it can be suggested that the Me_6-clusters have an extremely high polarizing power, and the main factor affecting the ligand-cluster interactions is the anion distance from the cluster center. As will be shown below, this distance is closely related to ligand bonding.

Anion Charge versus the Distance from the Cluster Center. Figure 4 presents the charge (bond valence sum) of chalcogen and halogen ions in various Mo_6 and Re_6 cluster compounds as a function of the ligand distance from the cluster center. As was mentioned above, in Chevrel phases, which have no outer ligands, the nonuniform charge is related to the structurally different X_1 and X_2 anions (the upper part of Figure 4a). Remarkably, change in the position of the S_2 anions in $GdMo_6S_8$ and $SnMo_6S_8$, as compared to that in Mo_6S_8, namely, its shift to the cluster center, agrees well with the charge redistribution found previously (Supporting Information, Figure 2S): The closer the ligand to the cluster center, the higher is its charge.

The same correlation exists for other Me_6-cluster compounds, but here the main difference in the anion charge and location is related to the inner and outer ligands. In fact, in spite of the similar lengths of the individual metal—ligand bonds, Me—X and Me—L, in the $Me_6X_8L_6$ structural units, the X atoms are ~0.8—1.3 Å closer to the cluster center than the L atoms, and their charges are obviously higher. Note that the crystal structure of some materials under study, such as $AgMo_6Br_{13}$, $Re_6Se_4Cl_{10}$, and $Re_6S_4Br_{10}$, is composed of two symmetrically independent clusters. As can be seen from Figure 4c, the charge distribution around the clusters (the data labeled as $AgMo_6Br_{13}$ and $AgMo_6Br_{13}'$, etc.) is very similar.

Thus, Figure 4 confirms the above analogy between the Me_6-cluster and a virtual cation with high polarizing power: According

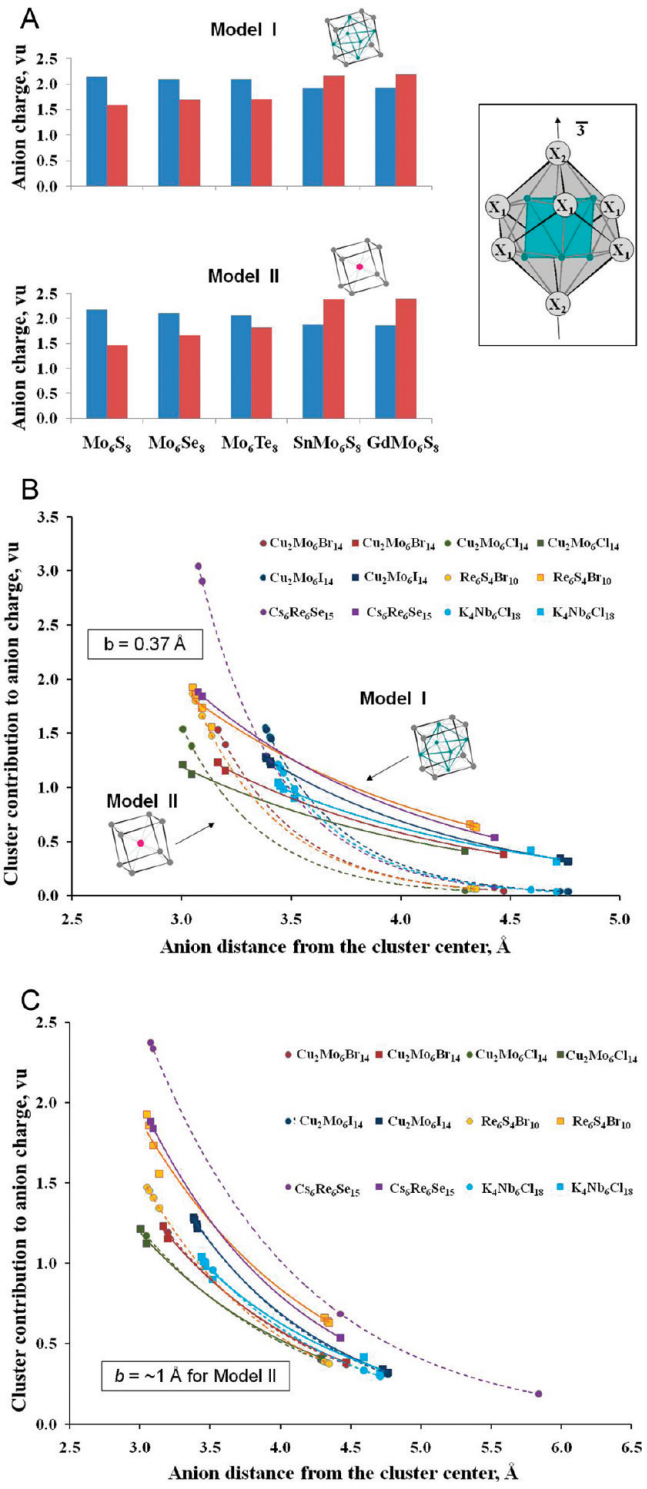

Figure 3. Bond valence calculations for models I and II: (a) Anion charge for two crystallographically different inner ligands, X_1 (in blue) and X_2 (in red), in Chevrel phases. The inset on the right side shows the ligand relation to the $\bar{3}$ symmetry axis. (b and c) Cluster contribution to the anion charge in a variety of cluster compounds vs ligand distancing from the cluster center (Calculations by model II were performed with bond valence parameter *b* equal to 0.37 and ~1 Å, respectively). Solid and dashed trendlines are related to models I and II, respectively. These lines were drawn assuming the exponential "charge-distance" response (see eq 1).

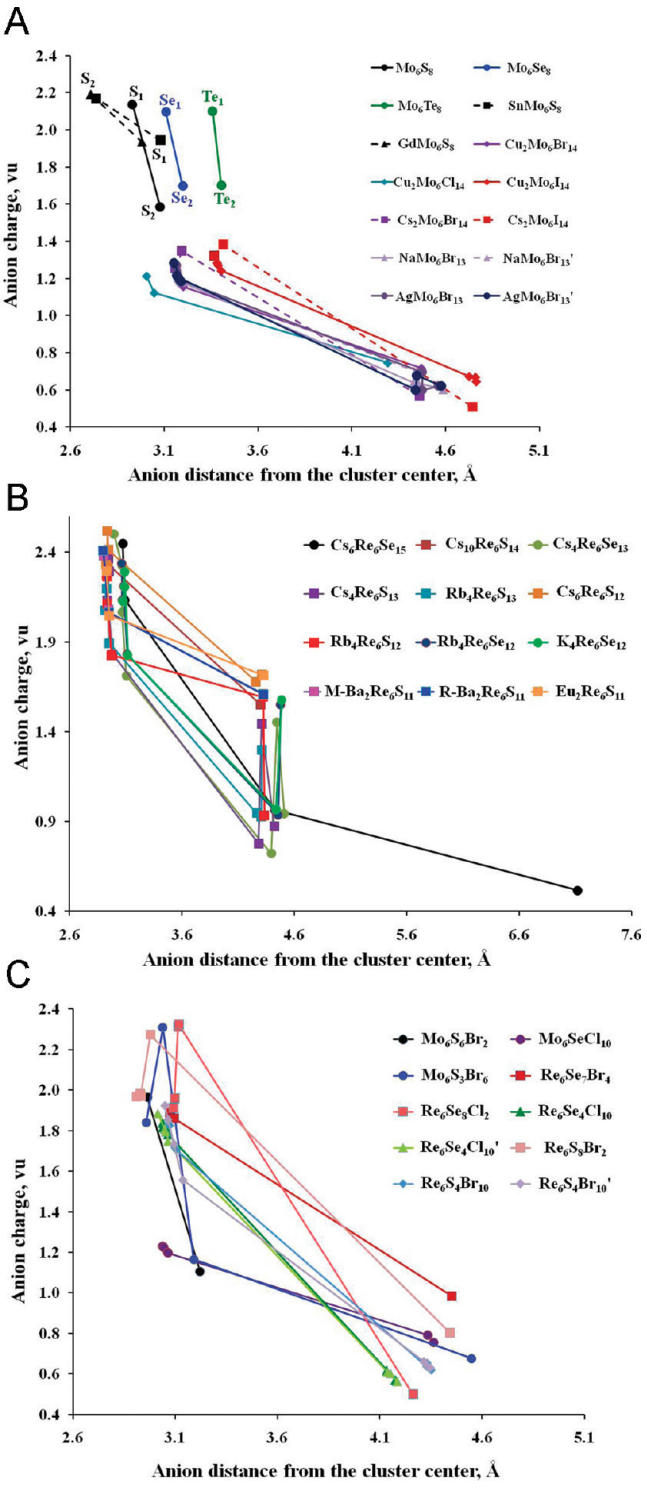

Figure 4. Distribution of the anion charge in a variety of cluster compounds as a function of the ligand distance from the cluster center: chalcogenides and halogenides with Mo_6- (a) and Re_6- (b) clusters; mixed chalcohalides with Mo_6- or Re_6- clusters (c).

to the charge-distance correlation, it is logical to suggest that the source of polarization around the cluster is located in its center. However, there is also a clear difference between the cluster and the common cations with a high charge/radius ratio: The deformability of the latter is typically very low, while the size and the shape of the Me_6-cluster are extremely sensitive to its charge,[3,11] external pressure,[11,25] and environment.[2b] For instance, Figure 5

dx.doi.org/10.1021/cm103617e |*Chem. Mater.* 2011, 23, 1901–1914

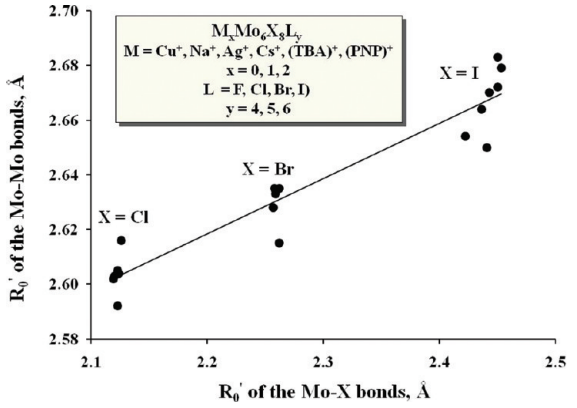

Figure 5. Cluster deformability in a variety of Mo_6-cluster halogenides: Correlation between the bond valence parameters calculated in this work for the Mo−Mo and Mo−X (X are inner ligands, Cl, Br, or I) bonds.

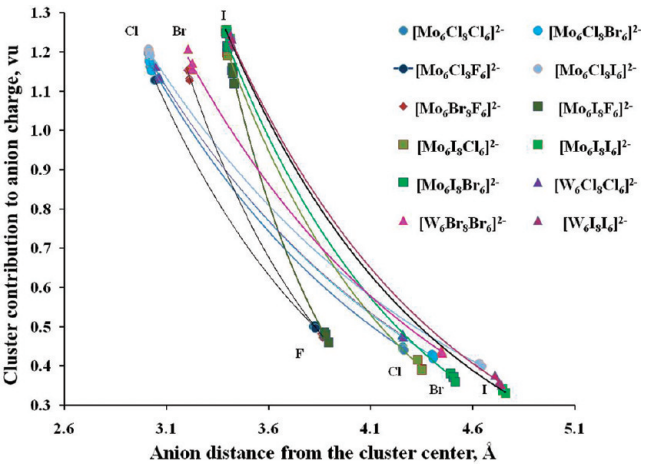

Figure 6. Effect of the cluster field on the distribution of the valence electrons between anions for a variety of metallo-organic halides: Me_6-cluster (Me = Mo, W) contribution to the anion (T = F, Cl, Br, I) charge vs ligand distance from the cluster center. The trendlines were drawn assuming the exponential "charge-distance" response.

presents the correlation between the bond valence parameters R_0' for the Mo−Mo bonds and those for the Mo−X bonds (X are inner ligands, Cl, Br, or I) for a variety of the Mo_6-cluster halogenides. As can be seen, the larger the anion cube around the cluster, the bigger is the cluster size. Hence, in spite of the high polarizing power, which is normally associated with "hard" cations, the cluster size is very flexible. Interestingly, the Mo_6-cation radius of ~1.3 Å (see estimation above) is significantly smaller than the distance of the Mo atoms from the cluster center, equal to ~1.8−2.0 Å (1.834, 1.842, and 1.847 Å for Mo_6Cl_{12}, 1.967 Å for Mo_6S_8), that is, the Mo atoms themselves may be polarized by the cluster electric field.

To emphasize the unusual nature of the anion charge distribution around the clusters, it can be compared with the structure of the electric double layer formed in the electrolyte solution near positively charged metal electrodes. In the anion part of the layer, the total negative charge decreases with the distance from the electrode surface. Similarly, the Me_6-cluster with high polarizing power creates a strong electrostatic field, in which the adjacent separate anions behave as part of a continuous dielectric medium, adjusting their charges to the distancing from the cluster center. The valence violations related to such adjustment are the cause of the material instability.

Comparison with Previous Results. It can be expected that the distribution of the valence charges between ligands presented in this study will be similar to the distribution of the effective charges around the clusters obtained by quantum chemical calculations (in spite of the obvious difference in their absolute values). In fact, Baranovsky et al.[26a,b] showed the high polarizability (domains of 55−65 $Å^3$) of the whole $Me_6X_8L_6$ structural unit (including the Me_6-core). Their conclusion was similar to ours: The essential difference in the effective charges for chemically identical anions arises from the existence of the internal electric field. However, they did not relate this field to the cluster, but to the additional cation groups. Another distinction between our results and those of quantum chemistry is related to the field distribution: The effective anion charges calculated, for example, by Arratia-Perez et al.[26c,d] for some of the Re_6, Mo_6, and W_6 cluster compounds were commonly higher for terminal ligands (see the data in the Supporting Information). Taking into account the ligand distance from the cluster center, such results can be interpreted as repulsion between the clusters and the anion electrons. In contrast, for our valence distribution we can speak about attraction of valence electrons by the cluster, which seems natural for the π-donor ligands.

Higher electron density for the terminal anions was suggested also by Tulsky et al.[27] based on the different chemical activity of these and inner ligands. However, the well-known[2,7] robust nature of the $[Me_6X_8]$ core in different solutions and high lability of the axial ligands testify rather to the opposite: the bond strengths (i.e., the valences) for the inner ligands should be significantly higher than those of the outer ligands. This can be confirmed by very simple estimation: close Me−X and Me−L distances, typical for the cluster compounds, are related to similar valences for each of these bonds (see eq 1). As the L and X ligands in the $Me_6X_8L_6$ units are commonly bonded to one and three Me cations, respectively, the cluster donation to the bond valence sum for the L anions (see eq 2) has to be almost three times lower than that for the X anions.

In fact, the maximal charge of the inner ligands in the Re_6 chalcogenides is about 2.4 vu, while the minimal charge of the outer ligands is close to 0.8 vu (Figure 4b). A similar ratio (1.2 vu/0.4 vu) can be seen in Figure 6, which presents the Me electron donation to the ligand charge for a variety of metallo-organic halides as a function of their distance from the cluster center. In addition, Figure 6 demonstrates nicely how higher ligand polarizability (I > Br > Cl > F) compensates the cluster field reduction, caused by a larger separation of the bigger anions from the cluster center. As a result of this compensation, there is no dramatic difference in the distribution of valence electrons for different anions, but the iodides should be less stable not only because of the weaker Mo−I bonding but also because of the increased inhomogeneity in the ligand charge. The estimation presented here takes into account only the metal−ligand interaction in separate $[Me_6X_8L_6]^{2-}$ units (the comparison is valid because of the same total charge (−2) of the units). Below we will see the effect of other structural parameters on the anion charge distribution.

Valence Violation and Structure Instability. As was remarked by Lee et al.[7h] in their review, the existence of broad families of cluster structures in the solid state might be at first sight surprising because of their almost axiomatic instability (Note that, in the absence of clear thermodynamic data for cluster

compounds, a common criterion of the material stability is the difficulty of its preparation. For example, Mo_6S_8 cannot be prepared by direct solid state synthesis, but only by metal extraction from more stable compounds like $NiMo_6S_8$ or $Cu_2Mo_6S_8$). A comparison of bonds in these and known stable materials might be even more astonishing, because these bonds seem to be very similar. For instance, in Chevrel phases, the lengths of the Mo−Mo bonds, which change from 2.65 to 2.86 Å,[3a] are obviously close to that of the Mo metal (2.78 Å). As was shown above (Figure 2), the Me−T bonds in cluster compounds are even stronger than those in common ionic solids. The question arises: What is the origin of cluster compounds′ instability, for example, why is Mo_6S_8 metastable, in contrast to very stable mineral molybdenite, MoS_2?

It was commonly accepted to correlate the material stability to the Me_6-cluster shape.[3] According to Yvon,[3a] the cluster symmetry increases with the cluster electron number, that is, the compounds with VEC = 24 should be the most stable. However, the synthetic studies seem to be in contradiction with this statement: For such cations as Li^+, Na^+, Mg^{2+}, Cd^{2+}, and so forth, it is relatively simple to obtain the Chevrel phases, $M^{n+}{}_xMo_6T_8$, with nx =1 or 2 by the direct high temperature synthesis, but compounds with nx =4 can be prepared only by chemical or electrochemical cation insertion into the Mo_6T_8 (T = S, Se) hosts at ambient temperatures.[5c] Moreover, the constant VEC = 24 is associated with a wide variety of cluster compounds with completely different stability; thereby it seems clear that the cluster VEC and shape are not the major factors in this case. In the previous work,[11] we have shown a good qualitative correlation between stability of Chevrel phases and anion valence violation, which was found to be minimal for nx =1 or 2. Thus, it is logical to suggest that the valence violations in the anion cluster environment are responsible of the material instability.

Numerous synthetic works of the past few decades showed different ways of structure stabilization such as insertion of additional cations between the cluster units or inside the clusters; partial chalcogen/halogen substitution; cluster units′ linkage by chalcogen groups with reduced oxidation state, and substitution of terminal ligands by organic groups. However, the effectiveness of these methods was rather sporadic, "with only limited rational planning"[7h] because of unknown structural mechanism of stabilization. In the subsequent parts it will be show that this mechanism can be understood as a minimization of valence violations.

■ DIFFERENT MODES OF STRUCTURE STABILIZATION

Cation Insertion. The most obvious way to change the nonuniform charge distribution on the ligands is by the insertion of additional cations between the structural units. It can be expected that the polarizing power of these cations will partially balance the strong electrostatic field formed by the cluster. To illustrate the effect of cation insertion for Chevrel phases on the valence distribution, Figure 7 presents separately the electron donation from the additional cations (area marked by gray) and that from the Mo atoms of the cluster to the anion charge (bond valence sum) as a function of VEC. As can be seen, the minimal valence violation for S and Se is associated with the insertion of a single mono or divalent cation per formula unit (VEC = 21 or 22), and such Chevrel phases are commonly the most stable.[3,11]

To demonstrate the effect of cation insertion on the valence distribution in other cluster compounds (case of constant VEC = 24), Figure 8 presents the electron donation of the M-cations (in red)

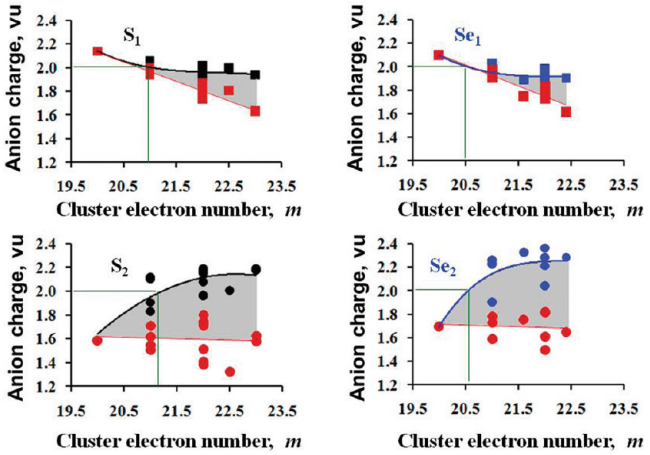

Figure 7. Redistribution of valence electrons, caused by cation insertion, for two crystallographically different anions in Chevrel phases, $M_xMo_6X_8$ (X = S, Se) as a function of the cluster electron number (VEC). The spots are the values calculated for different compounds. The anion charge (bond valence sum) of sulfur and selenium are marked by black and blue, respectively. The valence contribution of the Mo_6-clusters to the ligand charge is shown in red. The gray area is the cation input to the anion charge. The VECs related to the minimal valence violation (anion charge of 2 vu) are marked by green lines.

and the Mo atom (in green) to the charge (in blue) of crystallographically different anions in six materials, with the general formula $M_xMe_6T_{14}$. Since the bond valence sum depends mostly on the ligand coordination, we added the number of the Me−T bonds to the commonly used upper indexes "i" (inner) and "a" (outer) in the chemical symbols (the lower index indicates the crystallographically different anions). As can be seen, the cluster-ligand coordination in all six compounds is the same. In $Cu_2Mo_6T_{14}$ (T = Cl, Br, I), the selective contribution of the Cu^+ cations into the bond valence sum of the outer ligands results in increased homogeneity in the anion charge: The global instability index changes from 0.18 for the chloride to 0.23 for the iodide. In contrast, a Cs^+ ion inserted into similar structures contributes not only to the charge of the outer ligands but also to the inner ones. This leads to the less homogeneous distribution of the valence electrons between the ligands and high instability index (GII = 0.26−0.34 vu). Thus, this mode of material stabilization is especially effective when the inserted cation is bonded only to the outer ligands.

Increasing Connectivity of Structural Units. In the $M_xMe_6T_{14}$ compounds discussed above, the separated Me_6T_{14} units are linked to each other by inserted cations or cation groups. More frequently, the cluster units are interconnected by common anion or anion groups. Three different types of cluster linkages are presented in Figure 9a (additional linkage modes by anion groups will be discussed below): The bridging anion may be (i) in the apical position for the two adjacent clusters ($L^{2(a\text{-}a)}$); (ii) in the apical position for one of the clusters, but in the inner position for the adjacent one ($L^{4(i\text{-}a)}$); and (iii) in the inner position for both clusters ($L^{6(i\text{-}i)}$). The number of Me-atoms bonded to the bridging anion is two, four, and six, respectively (see the number in the upper index of the ligands). A higher coordination number results in a larger electron donation by the Me-atoms to the anion charge (bond valence sum).

For instance, in the layered compound, Mo_6Cl_{12}, the terminal ligands, $Cl_3{}^{1a}$ and $Cl_4{}^{2(a\text{-}a)}$, are bonded to one and two clusters,

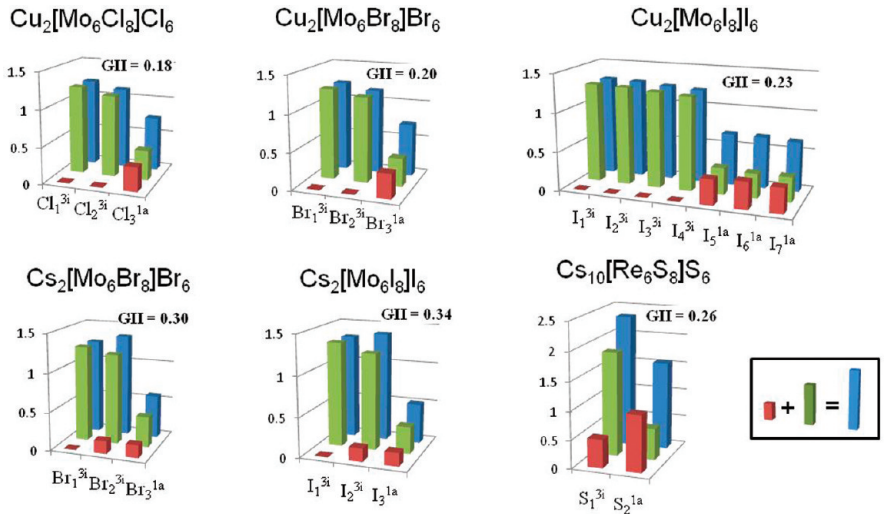

Figure 8. Distribution of the valence electrons on the ligands in the $M_xMe_6T_{14}$ compounds and the global instability index (GII). The inset shows that the total anion charge (in blue) is balanced by the sum of the cation and cluster contributions marked by red and green, respectively. The X and Y axes represent crystallographically independent anions with different connectivity and their valence (in vu), respectively.

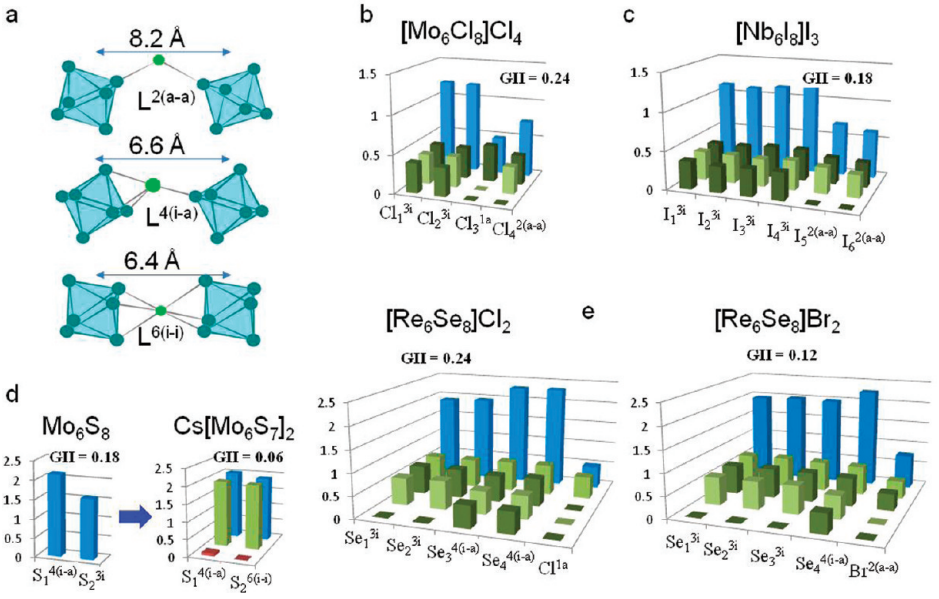

Figure 9. Effect of the unit connectivity on the valence distribution and the global instability index (GII): (a) Three types of the cluster linkages. (b−e) The valence contribution from cations (in red) and from the cluster (in green) to the ligand charge (in blue). For Mo_6Cl_{12}, Nb_6I_{11}, $Re_6Se_8Cl_2$, and $Re_6Se_8Br_2$, the input of each Me atom bonded to the ligand is shown separately (different types of green color are used for clarity). The X and Y axes are the same as in Figure 8.

respectively. As a result, the $Cl_4^{2(a-a)}$ charge is twice as much as that of Cl_3^{1a} (Figure 9b). In Nb_6I_{11}, with a three-dimensional cluster linkage, all the terminal ligands are of the bridging type $L^{2(a-a)}$. Consequently, their charge is relatively high (Figure 9c). In both compounds, the direct connection between the clusters results in a more homogeneous charge distribution and material stabilization: GII is equal to 0.24 vu for Mo_6Cl_{12} and 0.18 vu for Nb_6I_{11}. In $CsMo_{12}S_{14}$, the linkage of the cluster units is very similar to that in Chevrel phases. The difference is that the S_2 anion is not bonded to one cluster, but is shared by two adjacent clusters, that is, its coordination number changes from three to six: $S_2^{3i} \rightarrow S_2^{6(i-i)}$. Because of the higher connectivity, the GII decreases from 0.18 vu for Mo_6S_8 to 0.06 vu for $CsMo_{12}S_{14}$ (Figure 9d). In this case, the $S_2^{6(i-i)}$ connectivity results in a superposition of electrostatic fields existing around two interconnected clusters. Consequently, the fields partially cancel one another in the points equidistant from both clusters (Note that the $L^{2(a-a)}$ and $L^{6(i-i)}$ linkages are highly symmetric. For example, the separation between the bridging anions and the two clusters is 4.33 and 4.35 Å for Mo_6Cl_{12}, 4.94 and 5.00 or 2 × 4.91 Å for Nb_6I_{11} and 2 × 3.19 Å for $CsMo_{12}S_{14}$).

However, in some compounds the higher connectivity of the structural units increases the difference in the ligand bonding. For example, as we saw above, the nonuniform distribution of the valence electrons around the cluster in the Chevrel phase, Mo_6S_8, is related to the different bonding of the two inner anions, $S_1^{4(i-a)}$ and S_2^{3i} (Figure 9d). A similar effect takes place in the layered $Re_6Se_8CI_2$, where additional bonding in the Re_6-cluster layers

dx.doi.org/10.1021/cm103617e |*Chem. Mater.* 2011, 23, 1901–1914

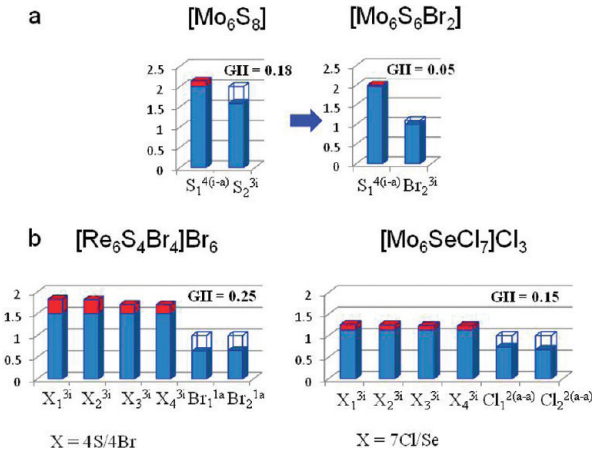

Figure 10. Effect of the chalcogen-halogen arrangement on the violated anion charge: (a) Substitution of two sulfur atoms (marked as X_2 in the inset of Figure 2a) for Br in the Chevrel phase, Mo_6S_8. (b) Two compounds with purely halogen outer ligands and random chalcogen-halogen distribution in the inner ligands. The filled columns (in blue or blue plus red) present the total anion charge (bond valence sum); their red part shows the valence excess as compared to the formal oxidation state; the empty part is the valence deficiency. The X and Y axes are the same as in Figure 8.

increases the inhomogeneity of the ligand charge and destabilizes the material: GII = 0.24 (Figure 9e, left). In contrast, the bond rearrangement ($S_3^{4(i\text{-}a)} \rightarrow S_3^{3i}$; $Cl^{1a} \rightarrow Br^{2(a\text{-}a)}$) associated with the formation of cluster chains in $Re_6Se_8Br_2$ (Figure 9e, right) and $Re_6S_8Br_2$ results in structure stabilization: GII = 0.12.

It seems that the opposite influence of the $L^{4(i\text{-}a)}$ connectivity on the anion charge as compared to that of the $L^{2(a\text{-}a)}$ and $L^{6(i\text{-}i)}$ linkages arises from the asymmetry of the former. In fact, in Mo_6S_8 the bridging $S_1^{4(i\text{-}a)}$ anion is much closer to one of the clusters than to the other: The distances are 2.93 and 4.39 Å, respectively. In $Re_6Se_8CI_2$, the distances of the bridging $Se_3^{4(i\text{-}a)}$ and $Se_4^{4(i\text{-}a)}$ anions from one of the cluster are 3.11 and 3.12 Å, while those from the second cluster are 4.46 and 4.50 Å. Thus, the interactions of the bridging anion with one of the clusters should be fundamentally stronger, that is, the clusters' fields cannot cancel each other out.

Mixed Chalcogenide/Halide Compounds. One of the unusual properties of the cluster compounds is the straightforward formation of mixed chalcohalides. In the latter, divalent chalcogen and monovalent halogen ions may be substituted for each other, but they also show a clear tendency for maximal separation on the inner and outer ligands, respectively.[7a,f] We did not find any plausible explanation for this phenomenon in previous studies devoted to these compounds. However, the atomic arrangement can be simply understood as the ligand adjustment to the strong electrostatic field of the cluster: It is clear that a minimum violation from the formal oxidation state should be realized in compounds, where chalcogens (−2) and halogens (−1) will be located close to and far away from the cluster, respectively.

A well-documented example is the stabilization of the Chevrel phase, Mo_6S_8, by halogen in compounds such as $Mo_6S_6X_2$ (X = Br, I).[25] In the earlier works[3,25] it was assigned to the higher VEC (20 and 22 vu, respectively), but recently[11] we have shown that the replacement of one type of sulfur anions (S_2) by Br is related to a dramatic decrease in the valence violation (Figure 10a): The global instability index, GII, changes from 0.18 vu for Mo_6S_8 to 0.05 vu for $Mo_6S_6Br_2$. Another example is the existence of the mixed compounds with the general formula $Re_6Q_{8-n}Y_{2+2n}$ (n = 0−4). Three of these materials, $Re_6Se_8CI_2$, $Re_6Se_8Br_2$, and $Re_6S_8Br_2$, were discussed above (Figure 9e). For all of them, the inner and outer ligands are presented by the chalcogen and halogen atoms, respectively, while their charges of 1.9−2.3 vu (for S or Se) and 0.5−0.8 vu (for Cl or Br) are convenient for the valence electron gradient existing around the clusters.

Figure 10b shows the bond valence sums and the valence violation for anions in two additional materials, $Re_6S_4Br_{10}$ and Mo_6SeCl_{10}, where divalent chalcogen and monovalent halogen ions are randomly distributed between the inner sites. Because of the difference in the anion charges, such substitution should be problematic for common ionic compounds. However, as we saw above, the area between the clusters has a flexible density of valence electrons, and thereby it allows for the $Q^{2-} - Y^{-}$ replacement. In fact, the bond valence sums of the inner ligands (∼1.7−1.8 vu for $Re_6S_4Br_{10}$ and ∼1.2 for Mo_6SeCl_{10}) are relatively close to the average formal oxidation state of the anion mixture (1.5 and 1.125 vu, respectively). Outer ligands with charges of ∼0.6 and 0.7 vu are presented by monovalent halogen. As a result, the global instability index, GII, of these compounds is relatively low (0.25 and 0.15 vu, respectively), especially for the latter compound with a higher connectivity of the outer ligands.

Changes in the Formal Oxidation State of Chalcogen Atoms. As was mentioned above, the cluster units can be linked by additional chalcogen groups. The typical feature of the latter is the unusual oxidation states of the chalcogen, when the total charge of the whole group, consisting of two, three, or even seven atoms, is equal to −2. As far as we know, the origin of this phenomenon was not discussed in previous studies, but, as in the case of mixed chalcohalides, it can be easily understood as one of the ways of minimization of valence violations. In fact, the area between the clusters with a distance of more than 4 Å from their centers is the region of low density of valence electrons, which should be very favorable for the formation of the unusual anion groups.

For instance, in $Cs_6Re_6S_{12}$, the formal oxidation state of all sulfur anions is −2, and the calculation shows a strong valence violation (GII = 0.45), especially for the nonbridging terminal ligand S_7^{1a} (Figure 11a). In contrast, in the selenides, $M_4Re_6Se_{12}$ (M = Rb, K, Tl), the Se_5^{1a} anions form the $(Se_2)^{2-}$ pair, connecting two adjacent clusters (Figure 11b). A similar $(S_2)^{2-}$ pair exists in the sulfide, $Rb_4Re_6S_{12}$. As a result, the GII of these compounds are relatively low (Table 1). In compounds such as Re_6Te_{15} and $Re_6Se_8Te_7$, the clusters are bridged by seven covalently bonded Te atoms, which form the quasi-planar butterfly like configuration with a total charge of −2. To use the bond valence model, we presented this linker as a Te^{2+} cation surrounded by two $(Te_3)^{2-}$ groups, with the structural formula $Te^{2+}[Re^{3+}{}_6Te^{2-}{}_8]^{2+}(Te_3)^{2-}{}_2$. Such a presentation might seem artificial, but it agrees well with the "distance-charge" correlation found in this work: the distances of crystallographically different anions from the Re_6-cluster center in Re_6Te_{15} are 3.3 Å for the inner ligands, 4.6 Å for the outer ligands, and 6.5 Å for the central atom in the butterfly group. The bond valence calculations performed in accordance with this structural formula result in a relatively low GII of 0.22 vu (Figure 11c).

An interesting case of ligand charge adjustment to the cluster field can be found in the crystal structure of $Cs_4Re_6S_{13.5}$, determined by Bronger et al.,[18e] who described the cluster linkage in this compound as a combination of two S^{2-}, three $(S_2)^{2-}$, and one $(S_3)^{2-}$ bridges (See ref 2a, p 1593). In our calculations, we replaced the triatomic $(S_3)^{2-}$ group by a S^{2+} cation coordinated

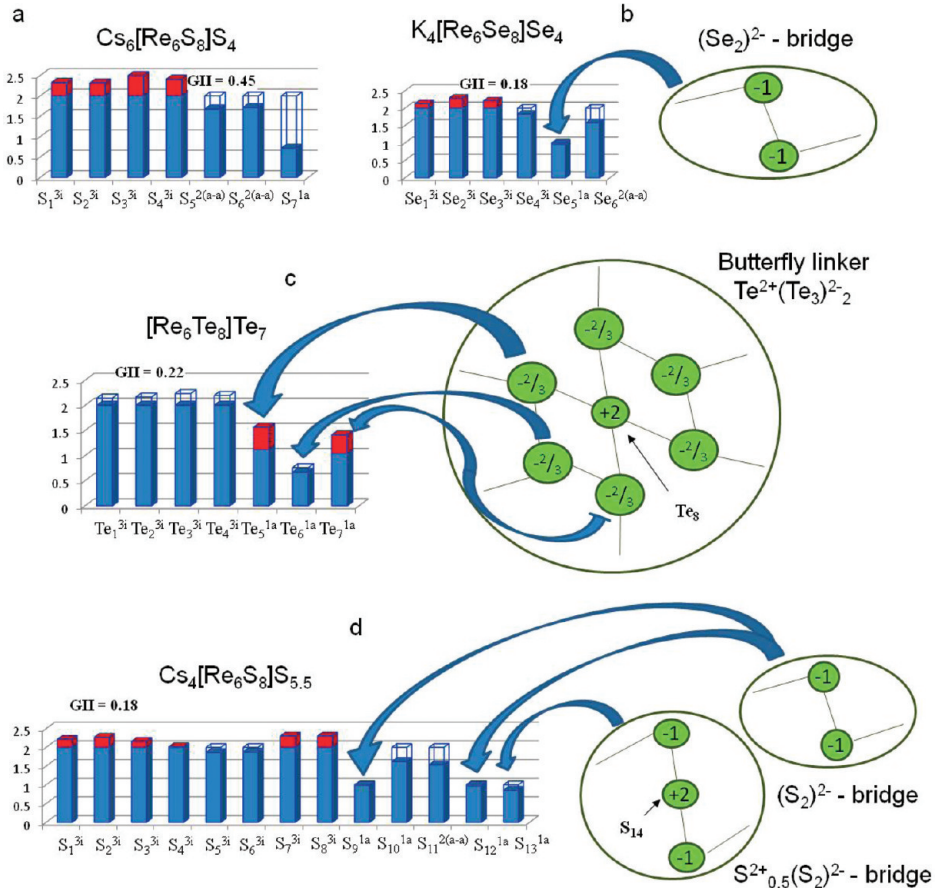

Figure 11. Effect of the reduced oxidation state of chalcogen atoms in the cluster linkers on the violated anion charge: Two compounds of similar stoichiometry with nonreduced (a) and reduced (b) oxidation state of chalcogen atoms. (c, d) Two compounds with complex cation−anion presentation of chalcogen bridges. The insets show the linker structure. The presentation style is the same as in Figure 10.

by two monovalent sulfurs (Figure 11d), with the structural formula $Cs^{+}_{4}S^{2+}_{0.5}[Re_6S_8](S^{2-})_2(S^{-})_3$. Such a presentation agrees with the distancing of the crystallographically different sulfur atoms from the cluster center (2.9−3.0 Å for the inner ligands; 4.2−4.4 Å for the outer ligands and 5.3−5.4 Å for the S^{2+} cation), resulting in a relatively low GII of 0.18 vu. Note also that a partial occupation of the site in the crystal structure (occ = 0.5), found by Bronger et al.[18e] for the central atom in the triatomic group, is typical for cations, but not for anions.

Thus, the bond valence analysis allows for the determination of a stabilization mechanism in any cluster compound of this type. For instance (Figure 12), in $AgMo_6Br_{13}$ (GII = 0.23) two of the terminal ligands, Br_5^{1a} and Br_6^{1a}, are stabilized by cation insertion, while the third ($Br_7^{2(a-a)}$) is common for the two adjacent clusters. In $Eu_2Re_6S_{11}$, a favorable combination of the cluster linkage and the cation input into the charge of the terminal ligand, $S_3^{2(a-a)}$, results in a relatively homogeneous distribution of the valence electrons (GII = 0.15). In $Cs_4Re_6Se_{13}$ (GII = 0.24), the oxidation state of two terminal ligands, Se_5^{1a} and Se_7^{1a}, is reduced to −1 (structural formula $Cs^{+}_{4}[Re^{3+}_{6}Se^{2-}_{8}]\ [Se^{2-}(Se_2)^{2-}_{2}]$), while the third ($Se_6^{2(a-a)}$) is common for two clusters. In $Cs_6Re_6Se_{15}$, the terminal ligands, Se_3^{1a}, have a reduced oxidation state of −1 (structural formula $Cs^{+}_{6}[Re^{3+}_{6}Se^{2-}_{8}]\ [Se^{2-}(Se_2)^{2-}_{3}]$), but an unfavorable cation charge distribution, as well as the presence of an additional anion separated from the Re_6-cluster (Note that Se_4 atom is not connected to the cluster, but only to the Cs cations), results in a relatively high GII of 0.32 vu.

Compounds with $[Me_6X_{12}]$ Structural Units. As was mentioned in the Introduction, compounds with Nb or Ta clusters differ from those of Mo, Re, W, and so forth by the number of inner ligands: 12 instead of 8 (the exception is Nb_6I_{11} discussed above). The increase in the coordination number is possible because of the larger cluster dimensions. In fact, Table 1 shows that the bond valence parameter of the Me−Me bonds, $R_0'_{Me-Me}$, is equal to 2.76−2.77 Å for the Nb_6-chlorides (see data for $K_4Nb_6Cl_{18}$, $Li_2Nb_6Cl_{16}$, $LiNb_6Cl_{15}$) and only 2.60−2.61 Å for the Mo_6, Re_6, and W_6-chlorides (see data for Mo_6Cl_{12}, $Cu_2Mo_6Cl_{14}$, $(TBA)_2Mo_6Cl_{14}$, $Re_6Se_4Cl_{10}$, $(TBA)_2W_6Cl_{14}$). The larger dimensions are related to the weaker Me−Me bonds within the cluster: VEC = 16 instead of 24. The Me−ligand bonds for Nb in these compounds are also weaker than those for Mo, Re, and W. For instance, according to the data of Table 1, $R_0'_{Me-Cl}$ is equal to 2.20 Å for Nb, 2.12 Å for Mo and Re, and 2.14 Å for W.

In contrast to the $[Me_6X_8]$ structural units, each of the 12 inner ligands is bonded only to two Me-atoms: $X^{3i} \rightarrow X^{2i}$. This leads to the larger separation of the ligands from the cluster center (e.g., ∼3.0 and 3.5 Å for the chlorides with Mo_6- and Nb_6-clusters, respectively). It is clear that this change in bonding should result in a more homogeneous distribution of valence electrons between anions around the Nb_6-clusters: The cluster electron donation to the charge of the terminal ligands is only twice as small as that for the inner ligands (Compare with the 1:3 ratio for the $[Me_6X_8]L_6$ structural units). Thus, in the case of a similar connectivity between the clusters, compounds with

dx.doi.org/10.1021/cm103617e |*Chem. Mater.* 2011, 23, 1901–1914

$[Me_6X_{12}]$ units should be more stable than those with $[Me_6X_8]$ units (this estimation does not take into account the weaker Me−Me and Me−ligand bonds). In fact, as can be seen in Figure 13, GII is equal to 0.05 for $K_4Nb_6Cl_{18}$, 0.06 for $Li_2Nb_6Cl_{16}$, and 0.08 for $LiNb_6Cl_{15}$. These values can be compared respectively with GII = 0.18 for $Cu_2Mo_6Cl_{14}$ (Figure 8), GII = 0.23 for $AgMo_6Br_{13}$, and GII = 0.15 for $Eu_2Re_6S_{11}$ (Figure 12), because these compounds have a similar cluster connectivity.

Compounds with Centered Clusters. As was mentioned in the Introduction, octahedral clusters of Sc, Sr, or Zr are stable only in the presence of additional atoms in the cluster centers (Figure 1c). To illustrate the use of the bond valence model for such type of materials, we performed calculations for two of them, with the following structural formula: $Sc[CoSc_6I_{12}]$ and $[CoZr_6Cl_{12}]Cl_3$ (The Co atom is in the cluster center). In the former compound, six Sc atoms form the cluster, while the seventh atom in the formula unit is a normal Sc^{3+} cation located in the interstitial site between the $CoSc_6$-clusters. The cluster linkage is similar to that of Chevrel phases: One anion, I_1^{2i}, is in a simple inner position (two Sc−I bonds), while the second one, $I_2^{3(i-a)}$, is bonded to two clusters (the inner position with two Sc−I bonds for the closest cluster and the apical position for the adjacent cluster) (see the left-hand inset in Figure 13b). In $CoZr_6Cl_{15}$ the linkage is achieved by terminal ligands, which are common for two clusters (see the right-hand inset in Figure 13b).

If we use the presentation of the clusters as single virtual cations, the radii of the $CoSc_6$ and $CoZr_6$ cations should be about 2.1 and 1.8 Å, while their charges are 9 and 15 vu, respectively. Thus, the polarizing power of these "theoretical" cations q/r^2 should be equal to 2.0 e/Å^2 and 4.6 e/Å^2, and we can expect a relatively low anion polarization, especially around the $CoSc_6$ cluster. It should be emphasized that, for this structural type, the exact electron distribution inside the cluster is unknown. The Co atom in the cluster center can be formally regarded as an anion with an oxidation state of −9. In this case, all 9 cobalt electrons should be distributed between the Co−Sc or Co−Zr bonds, and they should not assist in the Sc−Sc or Zr−Zr bonding. This assumption results in $R_0'_{Sc-Sc}$ = 3.071 Å or $R_0'_{Zr-Zr}$ = 3.108 Å, as well as in the valences of 0.32 and 0.43 vu for the Sc−Sc bonds and 0.375 vu for the Zr−Zr bonds. The opposite limiting case is a full transfer of the valence electrons from the cobalt to six Sc or six Zr atoms, related to $R_0'_{Sc-Sc}$ = 3.328 Å or $R_0'_{Zr-Zr}$ = 3.365 Å, as well as the valences of 0.65 and 0.85 vu for the Sc−Sc bonds and 0.75 vu for the Zr−Zr bonds. The latter scheme is more expedient to the general model of cluster polarization (described above), where the positive charge is concentrated in the cluster center.

In any case, the uncertainty in the electron distribution inside the cluster does not affect the ligand charge calculations based on the known formal oxidation state of Sc^{3+} or Zr^{4+}. Figure 13b shows the relatively close bond valence sums for two crystallographically different anions in Sc_7CoI_{12} (GII = 0.09) and Zr_6CoCl_{15} (GII = 0.08). Such a distribution arises from the

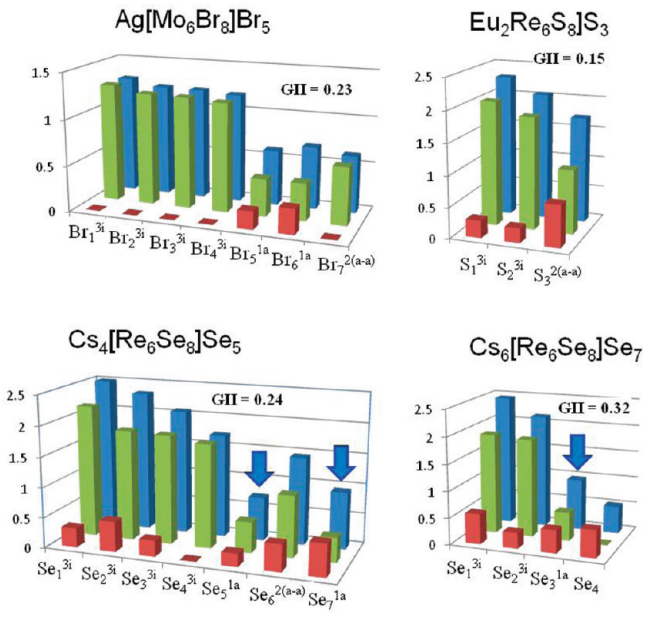

Figure 12. Complex effects of cation insertion, ligand linkage, and reduced oxidation state of chalcogens (the latter are marked by arrows) on the anion charge. The presentation style is the same as in Figure 8.

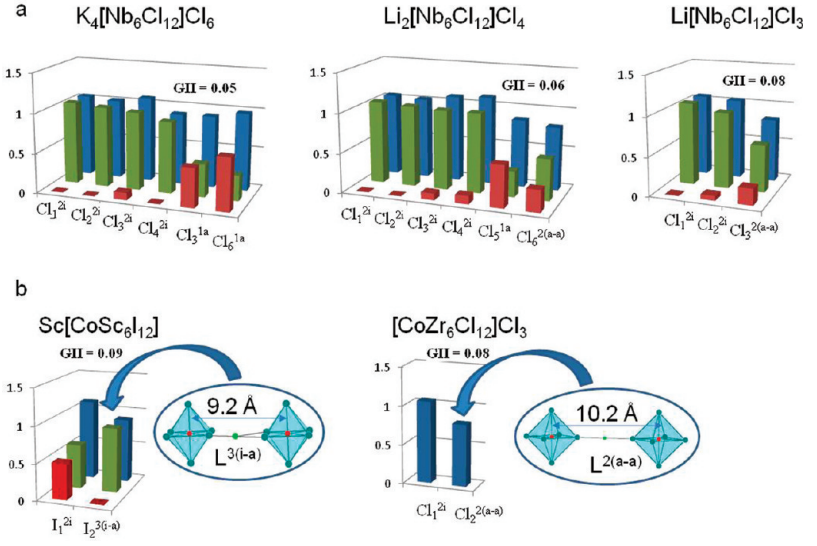

Figure 13. Distribution of the anion charge in compounds with $[Me_6X_{12}]$ (a) and $[ZMe_6X_{12}]$ (b) cluster blocks. The insets show the anion linkage. The presentation style is the same as in Figure 8.

dx.doi.org/10.1021/cm103617e |*Chem. Mater.* 2011, 23, 1901–1914

favorable bonding combinations. For Sc_7CoI_{12}, this is the additional charge transfer from the Sc^{3+} cation to the first anion, I_1^{2i}, and the bridging position of the second anion, $I_2^{3(i-a)}$. For Zr_6CoCl_{15}, the difference in the bond valence sums for the two anion types is not big because of the same bond number for the inner and apical bridging ligands. However, one can see the ligand polarization by cluster in this compound: The charge of the Cl_2 anion is clearly lower than that of the Cl_1 anion. This agrees with their distance from the cluster center: 5.09 and 3.58 Å, respectively.

CONCLUSIONS

In spite of the great previous efforts to understand the chemical bonding in the Me_6-cluster (Me = metal) compounds, this work shows for the first time the high polarizing power of the clusters. Because of the strong electrostatic field around the clusters, the adjacent separate anions behave as part of a continuous dielectric medium, adjusting the valence to their distance from the cluster center: The closer the anion to the cluster center, the higher is its charge. The study was based on a new approach: in contrast to the common bond description by the molecular orbital diagrams, we used the bond valence calculations, which allow to determine the charge of each separate anion (defined as its bond valence sum) in the crystal structure. The great advantage of such calculations is their simplicity: The method uses a fundamental relation between the bond lengths and their valences, and it needs only the knowledge of crystallographic data and cation charges. The calculations were performed for a wide variety of chalcogenides and halides with Mo_6 and Re_6 clusters. Compounds with other clusters were presented for comparison.

The study shows the importance of the discovered effect, namely, its influence on the structural and physical properties. It explains such unusual structural features of these compounds as the straightforward formation of mixed chalcohalides, anion ordering, or reduced oxidation state of chalcogen in the cluster linkers. The violated valences or lattice strains caused by anion polarization are the source of the material instability; thereby all the materials under study were characterized by the global instability indexes. Different structural ways of material stabilization were elucidated. We hope that this study will help to design new clusters compounds and to modify existing ones for uses such as catalysis, energy storage, and superconductivity.

ASSOCIATED CONTENT

Supporting Information. Additional data related to the bond valence analysis. This material is available free of charge via the Internet at http://pubs.acs.org.

AUTHOR INFORMATION

Corresponding Author
*E-mail: elenal@mail.biu.ac.il.

REFERENCES

(1) Cotton, F. A. *Inorg. Chem.* **1964**, *3*, 1217.

(2) (a) *Metal Clusters in Chemistry*; Braunstein, P., Oro, L. A., Raithby, P. R., Eds.; Wiley-VCH: Weinheim, Germany, 1999. (b) Prokopuk, N.; Shriver, D. F. In *Advances in Inorganic Chemistry*; Sykes, A. G., Ed.; Academic Press: San Diego, CA, 1999; Vol. 46, pp 1−49. (c) Gray, T. G. *Coord. Chem. Rev.* **2003**, *243*, 213.

(3) (a) Yvon, K. In *Current Topics in Material Science*; Kaldis, E., Ed.; Elsevier/North-Holland: Amsterdam, The Netherlands, 1979; Vol. 3. (b) *Topics in Current Physics: Superconductivity in Ternary Compounds I*; Fisher, Ø., Maple, M. B., Eds.; Springer-Verlag: Berlin, Germany, 1982. (c) Pena, O.; Sergent, M. *Prog. Solid State Chem.* **1989**, *19*, 165.

(4) (a) Aurbach, D.; Lu, Z.; Schechter, A.; Gofer, Y.; Gizbar, H.; Turgeman, R.; Cohen, Y.; Moskovich, M.; Levi, E. *Nature* **2000**, *407*, 724. (b) Levi, E.; Gofer, Y.; Aurbach, D. *Chem. Mater.* **2010**, *22*, 860.

(5) (a) Schollhorn, R. In *Inclusion Compounds*; Atwood, J. L., Ed.; Academic Press: London, U.K., 1984; Vol. 1. (b) Levi, E.; Gershinsky, G.; Aurbach, D.; Isnard, O.; Ceder, G. *Chem. Mater.* **2009**, *21*, 1390. (c) Levi, E.; Gershinsky, G.; Aurbach, D.; Isnard, O. *Inorg. Chem.* **2009**, *48*, 8751.

(6) Mihailovic, D. *Prog. Mater. Sci.* **2009**, *54*, 309.

(7) (a) Saito, T.; Imoto, H. *Bull. Chem. Soc. Jpn.* **1996**, *69*, 2403. (b) Mironov, Y. V.; Virovets, A. V.; Naumov, N. G.; Ikorskii, V. N.; Fedorov, V. E. *Chem.—Eur. J.* **2000**, *6*, 1361. (c) Gabriel, J.-C. P.; Boubeker, K.; Uriel, S.; Batail, P. *Chem. Rev.* **2001**, *101*, 2037. (d) Selby, H. D.; Roland, B. K.; Zheng, Z. *Acc. Chem. Res.* **2003**, *36*, 933.(e) Welch, E. J.; Long, J. R. in *Progress in Inorganic Chemistry*; Karlin, K. D., Ed.; John Wiley & Sons, Inc.: New York, 2005; Vol. 54, pp 1− 45. (f) Pilet, G.; Perrin, A. *C. R. Chim.* **2005**, *8*, 1728. (g) Cordier, S.; Kirakci, K.; Mery, D.; Perrin, C.; Astruc, D. *Inorg. Chim. Acta* **2006**, *359*, 1705. (h) Lee, S. C.; Holm, R. H. *Angew. Chem., Int. Ed. Engl.* **1990**, *29*, 840.

(8) (a) Hughbanks, T. *Prog. Solid State Chem.* **1989**, *19*, 329.(b) *Structural and electronic paradigms in cluster chemistry*; Mingos, D. M. P., Ed.; Springer-Verlag: Berlin, Heidelberg, Germany, 1997.

(9) (a) Corbett, J. D. *Inorg. Chem.* **2000**, *39*, 5178. (b) Simon, A. *Phil. Trans. R. Soc. A* **2010**, *368*, 1285.

(10) (a) Perrin, A.; Perrin, C.; Sergent, M. *J. Less-Common Met.* **1988**, *137*, 241. (b) Perrin, C. *J. Alloys Compd.* **1997**, *262−263*, 10.

(11) Levi, E.; Aurbach, D. *Chem. Mater.* **2010**, *22*, 3678.

(12) Brown, I. D. *The chemical bond in inorganic chemistry: the bond valence model*; Oxford University Press: New York, 2006.

(13) Brese, N. E.; O'Keeffe, M. *Acta Crystallogr.* **1991**, *B47*, 192.

(14) (a) Thorp, H. H. *Inorg. Chem.* **1992**, *31*, 1585. (b) Palenik, G. J. *Inorg. Chem.* **1997**, *36* (122), 3394–4888. (c) Thorp, H. H. *Inorg. Chem.* **1998**, *37*, 5690. (d) Palenik, G. J. *Can. J. Chem.* **2006**, *84*, 99.

(15) Corbett, J. D. *J. Solid State Chem.* **1981**, *37* (335), 39–56.

(16) (a) Gougeon, P.; Salloum, D.; Cuny, J.; Polles, L.; Floch, M.; Gautier, R.; Potel, M. *Inorg. Chem.* **2009**, *48*, 8337. (b) Schafer, H.; Schnering, H.-G.; Tillack, J.; Kuhnen, F.; Wohrle, H.; Baumann, H. *Z. Anorg. Allg. Chem.* **1967**, *353*, 281. (c) Peppenhorst, A.; Keller, H.-L. *Z. Anorg. Allg. Chem.* **1996**, *622*, 663. (d) Kirakci, K.; Cordier, S.; Perrin, C. *Z. Anorg. Allg. Chem.* **2005**, *631*, 411. (e) Wang, P.; Xu, W.; Zheng, Y.-Q. *Solid State Sci.* **2003**, *5*, 573. (f) Perrin, C.; Potel, M.; Sergent, M. *Acta Crystallogr., Sect. C* **1983**, *39*, 415. (g) Perrin, C.; Sergent, M.; Traon, F.; Traon, A. *J. Solid State Chem.* **1978**, *25*, 197. (h) Cordier, S.; Naumov, N. G.; Salloum, D.; Paul, F.; Perrin, C. *Inorg. Chem.* **2004**, *43*, 219.

(17) (a) Preetz, W.; Harder, K.; Schnering, H. G.; Kliche, G.; Peters, K. *J. Alloys Compd.* **1992**, *283*, 413. (b) Preetz, W.; Bublitz, D.; Schnering, H. G.; Sassmannshausen, J. *Z. Anorg. Allg. Chem.* **1994**, *620*, 234. (c) Bruckner, P.; Preetz, W.; Punjer, M. *Z. Anorg. Allg. Chem.* **1997**, *623*, 8.

(18) (a) Bronger, W.; Kanert, M.; Ioevenich, M.; Schmitz, D. *Z. Anorg. Allg. Chem.* **1993**, *619*, 2015. (b) Bronger, W.; Ioevenich, M.; Schmitz, D. *J. Alloys Compd.* **1994**, *216*, 25. (c) Bronger, W.; Ioevenich, M. *J. Alloys Compd.* **1994**, *216*, 29. (d) Bronger, W.; Miessen, H.-J.; Neugroschel, R.; Schmitz, D.; Spangenberg, M. *Z. Anorg. Allg. Chem.* **1985**, *525*, 41. (e) Bronger, W.; Ioevenich, M.; Schmitz, D.; Schuster, T. *Z. Anorg. Allg. Chem.* **1990**, *587*, 91. (f) Bronger, W.; Miessen, H.-J. *J. Less-Common Met.* **1982**, *83*, 29. (g) Bronger, W.; Miessen, H.-J.; Schmitz, D. *J. Less-Common Met.* **1983**, *95*, 275. (h) Bronger, W.; Schuster, T. *Z. Anorg. Allg. Chem.* **1990**, *587*, 74. (i) Bronger, W.; Koppe, C.; Schmitz, D. *Z. Anorg. Allg. Chem.* **1997**, *623*, 239. (j) Huan, G.; Greaney, M.; Tsai, P. P.; Greenblatt, M. *Inorg. Chem.* **1989**, *28*, 2448.

(19) (a) Klaiber, F.; Petter, W. *J. Solid State Chem.* **1983**, *46*, 112. (b) Harbrecht, B.; Selmer, A. *Z. Anorg. Allg. Chem.* **1994**, *620*, 1861. (c)

Fischer, C.; Alonso-Vante, N.; Fiechter, S.; Tributsch, H.; Reck, G.; Schulz, W. *J. Alloys Compd.* **1992**, *178*, 305. (d) Speziali, N. L.; Berger, H.; Leicht, G.; Sanjines, R.; Chapuis, G.; Levy, F. *Mater. Res. Bull.* **1988**, *23*, 1597. (e) Leduc, L.; Perrin, A.; Sergent, M. *Acta Crystallogr., Sect. C* **1983**, *39*, 1503. (f) Pinheiro, C. B.; Speziali, N. L.; Berger, H. *Acta Crystallogr., Sect. C* **1997**, *53*, 1178. (g) Leduc, L.; Perrin, A.; Sergent, M.; Traon, F.; Pilet, J. C.; Traon, A. *Mater. Lett.* **1985**, *3*, 209. (h) Perricone, A.; Slougui, A.; Perrin, A. *Solid State Sci.* **1999**, *1*, 657.

(20) Zietlow, T. C.; Schaefer, W. P.; Sadeghi, B.; Hua, N.; Gray, H. B. *Inorg. Chem.* **1986**, *25*, 2195.

(21) Imoto, H.; Simon, A. *Inorg. Chem.* **1982**, *21*, 308.

(22) (a) Simon, A.; Schnering, H.-G.; Schafer, H. *Z. Anorg. Allg. Chem.* **1968**, *361*, 235. (b) Bajan, B.; Meyer, H.-J. *Z. Anorg. Allg. Chem.* **1997**, *623*, 791. (c) Bajan, B.; Balzer, G.; Meyer, H.-J. *Z. Anorg. Allg. Chem.* **1997**, *623*, 1723.

(23) (a) Hughbanks, T.; Corbett, J. D. *Inorg. Chem.* **1988**, *27*, 2022. (b) Zhang, J.; Corbett, J. D. *Inorg. Chem.* **1991**, *30*, 431.

(24) (a) Adams, S. *Acta Crystallogr., Sect. B* **2001**, *57*, 278. (b) Brown, I. D. *Chem. Rev.* **2009**, *109*, 6858.

(25) Ehm, L.; Dera, P.; Knorr, K.; Winkler, B.; Krimmel, A.; Bouvier, P. *Phys. Rev. B* **2005**, *72*, 14113.

(26) (a) Baranovski, V. I.; Korolkov, D. V. *Polyhedron* **2004**, *23*, 1519. (b) Baranovski, V. I.; Korolkov, D. V. *Russ. Chem. Bull., Int. Ed.* **2005**, *54*, 2705. (c) Arratia-Perez, R.; Hernandez-Acevedo, L. *Chem. Phys. Lett.* **1997**, *277*, 223. (d) Arratia-Perez, R.; Hernandez-Acevedo, L. *J. Chem. Phys.* **1999**, *110*, 2529.

(27) Tulsky, E. G.; Long, J. R. *Chem. Mater.* **2001**, *13*, 1149.